Inorg. Chem. **1992**, *31*, 4575–4581

Geometry, Electronic Structure, and Coordination Ability of $[Cu(diN)(PH_3)_2]^+$ (diN = HN=CHCH=NH) at the Lowest Energy Triplet Metal-to-Ligand Charge-Transfer Excited State. A Theoretical Study

Shigeyoshi Sakaki,* Hiroki Mizutani, and Yu-ichi Kase

Department of Applied Chemistry, Faculty of Engineering, Kumamoto University,
Kurokami, Kumamoto 860, Japan

Received January 7, 1992

The ground state and the lowest triplet metal-to-ligand charge-transfer (MLCT) excited state of $[Cu(diN)(PH_3)_2]^+$ (diN = HN=CHCH=NH) are investigated with the ab initio MO method, where electron correlation is incorporated by the second-order Møller–Plesset perturbation theory. This complex is calculated to be pseudotetrahedral (pTd) at the ground state but planar (Pl) at the lowest triplet MLCT ($^3A_2$) excited state. In the MLCT ($^3A_2$) state, one α-spin electron is localized on the Cu d orbital and the other α-spin electron is on the diN π^*_1 orbital. The electron distribution around the Cu atom in this MLCT excited state resembles very much that in a similar Cu(II) complex, $[Cu(diN)(PH_3)_2]^{2+}$. H_2O coordination to $[Cu(diN)(PH_3)_2]^+$ is difficult at the ground state but easily occurs at the $^3A_2$ MLCT excited state. The H_2O binding energy at the MLCT excited state is calculated to be 19 kcal/mol. This result produces a theoretical support to a quenching mechanism of McMillin et al. proposed for the triplet MLCT excited state of such Cu(I) complexes as $[Cu(NN)_2]^+$ and $[Cu(NN)(PR_3)_2]^+$ (NN = 1,10-phenanthroline and its derivatives; PR_3 = tertiary phosphine).

Introduction

Photoinduced electron-transfer reactions of transition metal complexes are of great importance for the photochemical conversion and storage of solar energy,[1,2] in which $[Ru(bpy)_3]^{2+}$ (bpy = 2,2′-bipyridine) has been actively investigated as an efficient photosensitizer. Also, Cu(I) complexes involving such heteroaromatic ligands as 1,10-phenanthroline (phen) and its analogues are expected to be useful as photosensitizers because these Cu(I) complexes exhibit metal-to-ligand charge-transfer (MLCT) absorption bands in the visible to near-ultraviolet region and their lowest excited state is a triplet MLCT state like $[Ru(bpy)_3]^{2+}$. Photochemistry of these Cu(I) complexes has been investigated well,[3–6] and photoreduction of methylviologen has been successfully carried out with $[Cu(dpp)_2]^+$ (dpp = 2,9-diphenyl-1,10-phenanthroline),[7] $[Cu(dmp)(PPh_3)_2]^+$ (dmp = 2,9-dimethyl-1,10-phenanthroline),[8] and $[Cu(tmbpy)(PPh_3)_2]^+$ (tmbpy = 4,4′,6,6′-tetramethyl-2,2′-bipyridine).[8] The lifetime of these Cu(I) complexes, which is one of the important factors to determine photoreactivity, has been reported to be substantially shortened by solvent coordination to Cu(I) at the MLCT excited state; as shown in Scheme I,[3g,i] a solvent molecule can coordinate to Cu(I) not in the ground state but in the MLCT excited state, to form a five-coordinate complex, in which nonradiative decay is accelerated by several factors.[3] This proposal has been examined by elegant experiments including temperature and pressure effects on the lifetime of the excited state.[3c,f,g,h] Molecular orbital methods are also expected to be useful in investigating coordination ability, geometry, and electronic structure of the MLCT excited state.

In this work, ab initio MO calculations are carried out on the singlet ground state and the triplet MLCT excited one of $[Cu(diN)(PH_3)_2]^+$ (diN = HN=CHCH=NH), where diN is a model of such heteroaromatic ligands as phen and its derivatives. The aim of this work is to obtain various information on geometry, electronic structure, and solvent coordination to Cu(I) at both the ground state and the triplet MLCT excited one. It is our intention with this work to present a clear theoretical understanding of the triplet MLCT excited state of the Cu(I) complexes and to produce theoretical evidence that a solvent molecule such as H_2O can coordinate to Cu(I) not in the ground state but in the triplet MLCT excited state.

Computational Details

Ab initio restricted Hartree–Fock (RHF) MO and ab initio unrestricted Hartree–Fock (UHF) MO calculations are performed for the singlet ground state and the triplet MLCT excited one, respectively, by using the Gaussian 82 program.[9] Electron correlation is incorporated by use

---

(1) For instance: (a) Kalyanasundaram, K. *Coord. Chem. Rev.* **1982**, *46*, 159. (b) Juris, A.; Balzani, V.; Barigelletti, F.; Campagna, S.; Belser, P.; von Zelewsky, A. *Coord. Chem. Rev.* **1988**, *84*, 85. (c) De Armond, M. K.; Myrick, M. L. *Acc. Chem. Res.* **1989**, *22*, 364.

(2) The following papers reported the idea that $[Ru(bpy)_3]^{2+}$ can be applied to solar energy conversion: (a) Kirch, M.; Lehn, J.-M.; Sauvage, J.-P. *Helv. Chim. Acta* **1979**, *62*, 1345. (b) Pileni, M.-P.; Braun, A. M.; Gratzel, M. *Photochem. Photobiol.* **1980**, *31*, 423. (c) Kalyanasundaram, K.; Gfatzel, M. *Helv. Chim. Acta* **1980**, *63*, 478.

(3) (a) Breddels, P. A.; Berdowski, P. A. M.; Blasse, G.; McMillin, D. R. *J. Chem. Soc., Faraday Trans. 2* **1982**, *78*, 595. (b) Del Paggio, A. A.; McMillin, D. R. *Inorg. Chem.* **1983**, *22*, 691. (c) Blasse, G.; Breddels, P. A.; McMillin, D. R. *Chem. Phys. Lett.* **1984**, *109*, 24. (d) McMillin, D. R.; Kirchhoff, J. R.; Goodwin, K. V. *Coord. Chem. Rev.* **1985**, *64*, 83. (e) Casadonte, D. J.; McMillin, D. R. *Inorg. Chem.* **1987**, *26*, 3950. (f) Palmer, C. E. A.; McMillin, D. R. *Inorg. Chem.* **1987**, *26*, 3837. (g) Palmer, C. E. A.; McMillin, D. R.; Kirmaier, C.; Holten, D. *Inorg. Chem.* **1987**, *26*, 3167. (h) Crane, D. R.; DiBenedetto, J.; Palmer, C. E. A.; McMillin, D. R. *Inorg. Chem.* **1988**, *27*, 3698. (i) Stacy, E. M.; McMillin, D. R. *Inorg. Chem.* **1990**, *29*, 393.

(4) (a) Sakaki, S.; Koga, G.; Sato, F.; Ohkubo, K. *J. Chem. Soc., Dalton Trans.* **1985**, 1959. (b) Sakaki, S.; Satoh, T.; Ohkubo, K. *Nouv. J. Chim.* **1986**, *10*, 145. (c) Sakaki, S.; Hashimoto, S.; Koga, G.; Ohkubo, K. *J. Chem. Soc., Dalton Trans.* **1988**, 1641.

(5) Kunkely, H.; Vogler, A. *J. Am. Chem. Soc.* **1986**, *108*, 7211.

(6) (a) McGarvey, J. J.; Bell, S. E. J.; Bechara, J. N. *Inorg. Chem.* **1986**, *25*, 4327. (b) McGarvey, J. J.; Bell, S. E.; Gordon, K. C. *Inorg. Chem.* **1988**, *27*, 4001.

(7) Edel, A.; Marnot, P. A.; Sauvage, J.-P. *Nouv. J. Chim.* **1984**, *8*, 495.

(8) (a) Sakaki, S.; Koga, G.; Ohkubo, K. *Inorg. Chem.* **1986**, *25*, 2330. (b) Sakaki, S.; Koga, S.; Hashimoto, S.; Ohkubo, K. *Inorg. Chem.* **1987**, *26*, 1817.

(9) Binkley, J. S.; Frisch, M.; Raghavachari, K.; DeFrees, D.; Schlegel, H. B.; Whiteside, R.; Fluder, E.; Seeger, R.; Pople, J. A. *Gaussian 82*; Carnegie-Mellon Quantum Chemistry Archive; Carnegie-Mellon University: Pittsburgh, PA, 1983. Several routines for effective core potential calculations supplied by P. J. Hay have been added to this program by Dr. N. Koga and Prof. K. Morokuma.

0020-1669/92/1331-4575$03.00/0

Scheme I

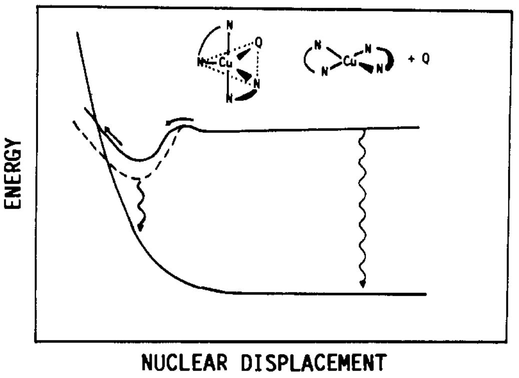

of second-order Møller–Plesset perturbation theory (MP2),[10] with all core orbitals frozen.

Because $[Cu(NN)(PR_3)_2]^+$ (NN = phen and its analogues) is too large to carry out ab initio MO calculations, $[Cu(diN)(PH_3)_2]^+$ is taken as its model, as shown in Chart I. Although diN seems too small compared to NN, diN has a N lone pair and π and π^* orbitals like NN. Actually, a reasonable MLCT excited state is calculated, as will be described later. Furthermore, several transition metal complexes involving substituted diimines, RN=CHCH=NR, have been reported.[11,12] Thus, diN is a reasonable model of NN, and semiquantitative discussion would be possible, at least, based on this model complex.

Two kinds of basis sets are employed in this work. The smaller one (hereafter called BS-I) is used in geometry optimization that is carried out with the energy gradient technique at the Hartree–Fock level. The larger one (hereafter called BS-II) is used in MP2 calculations. In BS-I, the inner core orbitals of Cu are replaced by an effective core potential[13] and its 3d, 4s, and 4p orbitals are represented by a (3s 2p 5d) primitive set contracted to [2s 2p 2d].[13] MIDI-1 sets are used for C, N, and O atoms, and the MINI-1 set is employed for P.[14] A (3s) primitive set is contracted to [2s] for H of diN and to a minimal basis set for H of PH_3.[15] In BS-II, MIDI-4 sets are used for C, N, O, and P atoms[14] and a (4s) primitive set contracted to [2s] is employed for H.[16] For Cu, a (13s 7p 4d) primitive set, which was proposed for the ^2D state of Cu,[13] is augmented with three p primitives to represent a valence 4p orbital[17] and one diffuse d primitive.[18] The resultant (13s 10p 5d) primitive set is contracted to [5s 4p 3d].

Chart I

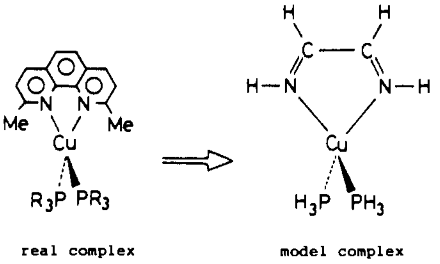

Table I. Mulliken Populations of $[Cu(diN)(PH_3)_2]^+$ at the $^1A_1$ Ground State and $^3A_2$ MLCT Excited State and of $[Cu(diN)(PH_3)_2]^{2+}$ at the $^2A_2$ State

	$[Cu(diN)(PH_3)_2]^+$				
	ground state		$^3A_2$ MLCT excited state		$[Cu(diN)(PH_3)_2]^{2+}$ $^2A_2$
	pTd	Pl	pTd	Pl	Pl
			ΔE^a (kcal/mol)		
MP2	0.0^b	16.5^c	75.3^d	69.2^e	280.2^f
Cu	28.38	28.34	27.99	27.98	28.02
PH_3	17.86	17.90	17.76	17.77	17.66
diN	29.90	29.87	30.48	30.49	29.67
			Spin Density		
d_{xz}			0.91	0.85	0.87
diN(π_y)			0.98	0.96	0

[a] Relative stability, where the pTd structure of the ground state is taken as the standard (energy 0). [b] E_t = −2508.748 47 hartrees. [c] E_t = −2508.7222 hartrees. [d] E_t = −2508.6284 hartrees. [e] E_t = −2508.6380 hartrees. [f] E_t = −2508.3020 hartrees.

Both planar (Pl) and pseudotetrahedral (pTd) structures are optimized at the singlet ground state and the triplet MLCT excited one, in which C_{2v} symmetry is adopted and a structure of PH_3 is taken from the experimental report.[19]

Results and Discussion

Ground State of $[Cu(diN)(PH_3)_2]^+$. Optimized geometries and Mulliken populations of both Pl and pTd structures are given in Figure 1 and Table I, respectively. The Pl structure is calculated to be less stable than the pTd one by ca. 16.3 kcal/mol at the MP2 level, according to our expectation. In fact, $[Cu(dmp)(PPh_3)_2]^+$ [20] and $[Cu(NN)_2]^+$ [21-29] take the pTd structure, reportedly. In some cases, a flattening distortion from tetrahedral structure has been reported for $[Cu(NN)_2]^+$, in which the dihedral angle is between 70 and 80°.[21-26,28] However, this flattening distortion is considered now to arise from a lattice effect due to stacking interaction of heteroaromatic ligands.[30,31] Thus, the

---

(10) (a) Reliability of the MP2 method depends on the kinds of transition metal elements. For instance, Ni(O) complexes cannot be successfully calculated with MP2-4 methods.[10b] In the case of Cu(I) complexes, however, the MP2 method yields similar results to that of the SD-CI method.[10c] (b) Sakaki, S.; Koga, N.; Morokuma, K. *Inorg. Chem.* **1990**, *29*, 3110. (c) Sakaki, S. To be published. For the reaction, $Cu^ICH_3 + CO_2 \rightarrow Cu(OCOCH_3)$, the exothermicity is calculated to be 43 kcal/mol at the Hartree–Fock level, 15 kcal/mol at the MP level, and 20 kcal/mol at the SD-CI level (after Davidson's correction), where double-ζ basis sets are used for all the elements.

(11) For instance: (a) Jardine, F. H. *Adv. Inorg. Chem. Radiochem.* **1975**, *17*, 115. (b) Leupin, P.; Schlapfer, C. W. *J. Chem. Soc., Dalton Trans.* **1983**, 1635. (c) Daul, C.; Schlapfer, C. W.; Goursot, A.; Penigault, E.; Weber, J. *Chem. Phys. Lett.* **1981**, *78*, 304. (d) Svoboda, M.; Dieck, H. T.; Kruger, C.; Tsay, Y.-H. *Z. Naturförsch.* **1981**, *36b*, 814. (e) Dieck, H. T.; Svoboda, M.; Greiser, T. *Z. Naturförsch.* **1981**, *36b*, 823. (f) Chaudret, B.; Koster, H.; Poilblanc, R. *J. Chem. Soc., Chem. Commun.* **1981**, 266. (g) Leupin, P.; Schlapfer, C. W. *J. Chem. Soc., Dalton Trans.* **1983**, 1635. (h) Porschke, K. R.; Bonrath, W.; Mynott, R. *Inorg. Chem.* **1990**, *29*, 5008.

(12) (a) Daul, C.; Schlapfer, C. W.; Goursot, A.; Penigault, E.; Weber, J. *Chem. Phys. Lett.* **1981**, *78*, 904. (b) Guimon, C.; Pfister-Guillougo, G.; Chaudret, B.; Poiblanc, R. *J. Chem. Soc., Dalton Trans.* **1985**, *43*. (c) Favre, P.; Schlapfer, C. W. *Chem. Phys. Lett.* **1987**, *139*, 250.

(13) Hay, P. J.; Wadt, W. R. *J. Chem. Phys.* **1985**, *82*, 270.

(14) Hujinaga, S.; Andzelm, J.; Kłobukowski, M.; Radzio-Andzelm, E.; Sakai, Y.; Tatewaki, H. *Gaussian basis sets for molecular calculations*; Elsevier: Amsterdam, 1984.

(15) Van Duizneveldt, F. B. Gaussian Basis Sets for the Atoms H-Ne for use in Molecular Calculations. *IBM J. Res. Dev.* **1971**, 945.

(16) Dunning, T. H., Jr.; Hay, P. J. *Methods of Electronic Structure Theory*; Schaefer, H. F., Ed.; Plenum: New York, 1977; p 1.

(17) Exponents and expansion coefficients were taken to be the same as the three most diffuse s primitives.

(18) (a) The exponent (ζ = 0.18) was determined by the even-tempered criterion. According to Hay,[18b] addition of a diffuse d function is recommended in the calculation of transition metal complexes. (b) Hay, P. J. *J. Chem. Phys.* **1977**, *66*, 4377.

(19) Herzberg, G. *Molecular Spectra and Molecular Structure*; Academic Press: New York, 1967; Vol. 3, p 610.

(20) Kirchhoff, J. R.; McMillin, D. R.; Robinson, W. R.; Powell, D. R.; McKenzie, A. T.; Chen, S. *Inorg. Chem.* **1985**, *24*, 3928.

(21) Hamalainen, T.; Turpeinen, U.; Ahlgren, M.; Raikas, T. *Finn. Chem. Lett.* **1978**, 199.

(22) Hamalainen, R.; Ahlgren, M.; Turpeinen, U.; Raikas, T. *Cryst. Struct. Commun.* **1979**, *8*, 75.

(23) Dessy, G.; Fares, V. *Cryst. Struct. Commun.* **1979**, *8*, 507.

(24) Burke, R. J.; McMillin, D. R.; Robinson, W. R. *Inorg. Chem.* **1980**, *19*, 1211.

(25) Burke, P. J.; Henrick, K.; McMillin, D. R. *Inorg. Chem.* **1982**, *21*, 1881.

(26) Hoffmann, S. K.; Corvan, P. J.; Singh, P.; Sethuleshmi, C. N.; Metzger, R. M.; Hatfield, W. E. *J. Am. Chem. Soc.* **1983**, *105*, 4608.

(27) Green, B. E.; Kennard, C. H. L.; Smith, G.; Elcombe, M. M.; Moore, F. H.; James, B. D.; White, A. H. *Inorg. Chim. Acta* **1984**, *83*, 177.

(28) Dobson, J. F.; Green, B. E.; Healy, P. C.; Kennard, C. H. L.; Pakawatchai, C.; White, A. H. *Aust. J. Chem.* **1984**, *37*, 649.

(29) Healy, P. C.; Engelhardt, L. M.; Patrick, V. A.; White, A. H. *J. Chem. Soc., Dalton Trans.* **1985**, 2541.

(30) Klemens, F. K.; Fanwick, P. E.; Bibler, J. K.; McMillin, D. R. *Inorg. Chem.* **1989**, *28*, 3076.

(31) Goodwin, K. V.; McMillin, D. R.; Robinson, W. R. *Inorg. Chem.* **1986**, *25*, 2033.

(32) Lippard, S. J.; Palenik, G. J. *Inorg. Chem.* **1971**, *10*, 1322.

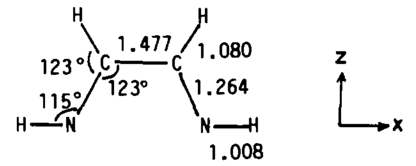

(A) Free diN

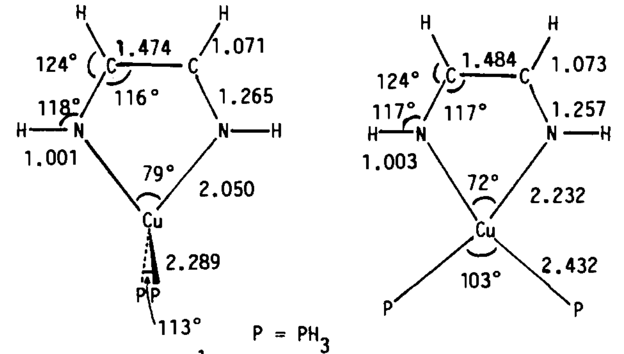

(B) $^1A_1$ Ground State

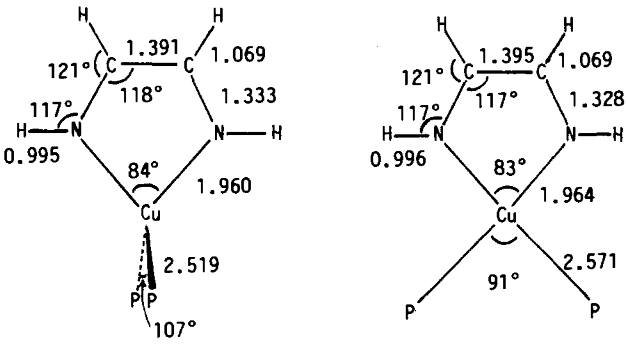

(C) $^3A_2$ MLCT Excited State

Figure 1. Optimized structures of the free diN and $[Cu(diN)(PH_3)_2]^+$ (bond distances in Å and bond angles in deg). These complexes adopt C_{2v} symmetry, meaning that they are symmetrical.

flattening distortion is not necessary to be considered here because the lattice interaction is not involved at all in MO calculations.

Although the experimental structure of $[Cu(diN)(PR_3)_2]^+$ has not been reported, the optimized structure of $[Cu(diN)(PH_3)_2]^+$ might be compared with experimental ones of similar complexes, $[Cu(phen)(PPh_3)_2]^+$ and $[Cu(dmp)(PPh_3)_2]^+$;[20] the optimized Cu–P distance (2.289 Å) is slightly longer than that (2.245–2.271 Å) of $[Cu(phen)(PPh_3)_2]^+$ but agrees well with that (2.282–2.305 Å) of $[Cu(dmp)(PPh_3)_2]^+$.[20] The optimized PCuP angle (113°) also agrees well with the experimental value (115.44°) of $[Cu(phen)(PPh_3)_2]^+$, while it is smaller than that (122.7°) of $[Cu(dmp)(PPh_3)_2]^+$.[20] The optimized Cu–N distance (2.05 Å) again agrees well with those of $[Cu(phen)(PPh_3)_2]^+$ and $[Cu(dmp)(PPh_3)_2]^+$. Although small differences are found between optimized values and experimental ones, these optimized Cu–P and Cu–N distances and PCuP angle are in the range of their experimental values reported for various Cu(I) complexes.[20–30] Considering that the phen, dmp, and PPh_3 ligands are replaced by the model ligands of diN and PH_3, these optimized values seem reasonable. The optimized structure of diN might be compared with the experimental one of dad in $[Ru(dad)_3]^{2+}$ (dad = 1,2-bis(*p*-methoxyphenyl)iminoethane).[11f,37] The optimized geometry of diN does not differ so much from dad's experimental structure in $[Ru(dad)_3]^{2+}$, except that diN in $[Cu(diN)(PH_3)_2]^+$ has slightly shorter C=N bonds and slightly longer C–C bonds than dad does. If we consider that the phenyl group in dad is substituted for H in diN, small differences in structure between diN and dad seem reasonable.

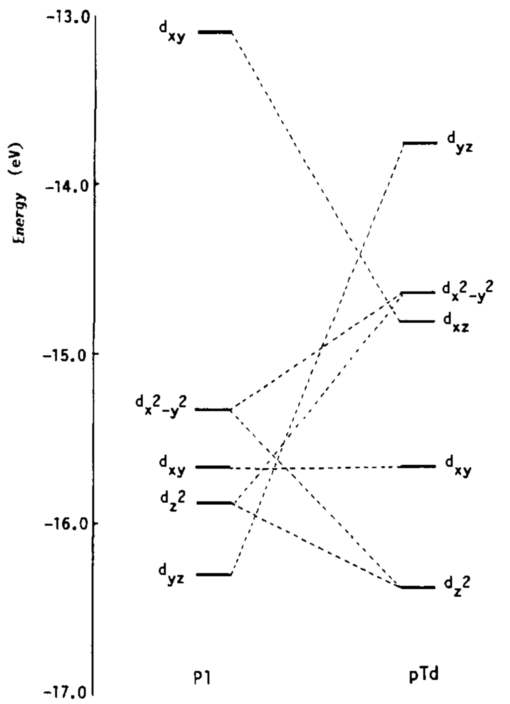

Figure 2. d-orbital energy levels at the $^1A_1$ ground state determined by using RHF-MO/BS-II calculations.

Now, let us explain the reason that the pTd structure is more stable than the Pl one at the ground state. As shown in Figure 2, the d_{xz} orbital is more destabilized in the Pl than in the pTd geometry. Because the d_{xz} orbital is doubly occupied at the ground state in both structures, the Pl is less stable than the pTd structure. Of course, steric factors would be the other reasons for the lesser stability of the Pl than the pTd structure because the former involves larger steric repulsion between two PH_3 and between diN and PH_3 than the latter.

Several interesting features are found in the structure of $[Cu(diN)(PH_3)_2]^+$. (1) Although bond distances in diN hardly change upon diN coordination to Cu(I), the NCC angle decreases by 6–7°, probably because electrostatic repulsion between two N lone pairs is reduced by diN coordination to Cu(I). (2) The C=N double bond hardly lengthens upon diN coordination to Cu(I), which suggests that back-donation from Cu to diN is not important in this complex; if back-donation contributes to the coordinate bond, the C=N distance should lengthen, because back-donation increases electron population on the diN π^*_1 orbital which is antibonding between C and N atoms (vide infra). This bonding nature is inconsistent with Mulliken populations; PH_3 and diN have positive Mulliken charges in $[Cu(diN)(PH_3)_2]^+$ (Table I), suggesting the importance of a donating interaction. (3) The Pl structure has longer Cu–P and Cu–N distances than the pTd does. This result is easily interpreted in terms of the trans-influence effect: diN and two PH_3 ligands occupy trans positions with respect to each other in the Pl structure, which lengthens both Cu–P and Cu–N distances in this structure. Of

---

(33) Lippard, S. J.; Melmed, K. M. *Inorg. Chem.* **1967**, *6*, 2223.

(34) Green, B. E.; Kennard, C. H. L.; Smith, G.; James, B. D.; White, A. H. *Acta Crystallogr., Sect. C: Cryst. Struct. Commun.* **1984**, *C40*, 426.

(35) Engelhardt, L. M.; Pakawatchai, C.; White, A. H.; Healy, P. C. *J. Chem. Soc., Dalton Trans.* **1985**, 125.

(36) Green, B. E.; Kennard, C. H. L.; Smith, G.; James, B. D.; Healy, P. C.; White, A. H. *Inorg. Chim. Acta* **1984**, *81*, 147.

(37) The experimental structure of $Ni(dad)_2$ has been also reported.[11d,e] However, the dad structure remarkably differs from that of $[Ru(dad)_3]^{2+}$, probably due to very strong back-donation from Ni(0) to dad. Because Cu(I) complexes are in general a weak d_π donors, the diN structure in $[Cu(diN)(PH_3)_2]^+$ is not appropriately compared with the dad structure in $Ni(dad)_2$.

Chart II

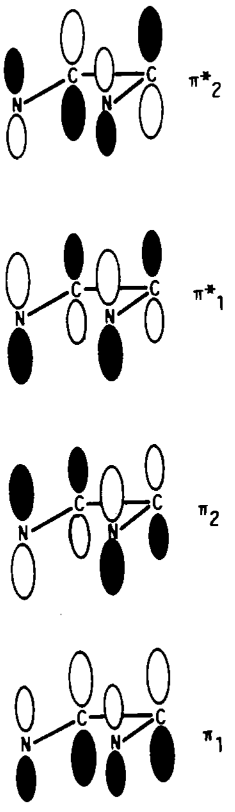

course, steric repulsion would contribute to the lengthening of these coordinate bonds. (4) In the Pl structure, the PCuP angle is larger than 90°, which is a normal value in a usual four-coordinate Pl structure. This result is easily understood by considering that the d^{10} configuration of Cu(I) does not require the PCuP angle to take 90° and that the steric repulsion between two PH_3 groups decreases upon increasing of the PCuP angle (vide infra).

Triplet MLCT Excited State of $[Cu(diN)(PH_3)_2]^+$. The diN ligand has two sets of π and π^* orbitals, as shown in Chart II. Because $[Cu(diN)(PH_3)_2]^+$ has C_{2v} symmetry, five d orbitals are classified into four representations. Thus, four kinds of MLCT excited states are formed by electron excitation from one of d orbitals to the diN π^*_1 (LUMO) orbital. Relative stabilities of these states are compared with each other in Table II.[38] In both the Pl and pTd structures, $^3A_2(d_{xz} \rightarrow \pi^*_1)$ is calculated to be the most stable. In the Pl structure, this result is easily understood because the d_{xz} orbital is the HOMO at the ground state (see Figure 2). In the pTd structure, on the other hand, the d_{yz} orbital is the HOMO at the ground state. Nevertheless, $^3A_1(d_{yz} \rightarrow \pi^*_1)$ is less stable than $^3A_2$. This result is easily explained by considering the coordinate bond of diN. In the $^3A_2$ state, the d_{xz} orbital is singly occupied and the d_{yz} orbital is doubly occupied, while in the $^3A_1$ state the d_{yz} orbital is singly occupied and the d_{xz} orbital is doubly occupied. Thus, the diN lone pair can donate electrons to the d_{xz} orbital in the $^3A_2$ state but cannot in the $^3A_1$ state.[39] Although electron donation from PH_3 to d_{yz} is more favorable in the $^3A_1$ state than in the $^3A_2$, electron donation from diN to Cu is more important than that from PH_3 to Cu in these MLCT excited states, because donating ability of diN is enhanced very much by one-electron excitation into its π^*_1 orbital (vide infra). Consequently, the $^3A_2$ state is more stable than the $^3A_1$ state, even though the d_{yz} orbital is the HOMO of the pTd structure at the ground state.

Table II. Relative Stabilities of Various Triplet MLCT Excited States (kcal/mol)

	Td			
	HF/BS-I[a]	HF/BS-II[b]	HF/BS-II[c]	MP2/BS-II[c]
$^3A_2(d_{xz} \rightarrow \pi^*_1)$	0.0	0.0	0.0	0.0
$^3A_1(d_{yz} \rightarrow \pi^*_1)$	4.9	11.9	11.6	13.8
$^3B_2(d_{x^2-y^2}$ or $d_{z^2} \rightarrow \pi^*_1)$	6.7	12.7		
$^3B_1(d_{xy} \rightarrow \pi^*_1)$	11.2	16.1		

	Pl			
	HF/BS-I[a]	HF/BS-II[b]	HF/BS-II[c]	MP2/BS-II[c]
$^3A_2(d_{xz} \rightarrow \pi^*_1)$	0.0	0.0	0.0	0.0
$^3A_1(d_{yz} \rightarrow \pi^*_1)$	20.7	33.6	28.9	41.1
$^3B_2(d_{x^2-y^2}$ or $d_{z^2} \rightarrow \pi^*_1)$	20.9	30.2		
$^3B_1(d_{xy} \rightarrow \pi^*_1)$	21.3	31.3		

[a] The geometry optimized at the $^1A_1$ state. [b] The geometry optimized at the $^3A_2$ state. [c] The $^3A_1$ state is compared to the $^3A_2$ state, where geometries of the former and the latter are optimized for the $^3A_2$ and $^3A_1$, respectively.

Relative stabilities and Mulliken populations are compared between the Pl and pTd structures in Table I. It is noted that the Pl structure is more stable than the pTd one at the $^3A_2$ MLCT excited state unlike the ground state. This reason will be clear in the following discussion.

Several interesting features are found in the optimized structures. (1) As shown in Figure 1, the C–N distance lengthens but the C–C distance shortens upon going to the $^3A_2$ MLCT excited state from the ground state. These geometrical changes in diN arise from one-electron excitation into the diN π^*_1 orbital (see Chart II). The π^*_1 orbital is antibonding between C and N atoms but bonding between two C atoms. Because the $^3A_2$ MLCT excited state is formed by one-electron excitation from Cu d_{xz} to diN π^*_1, this MLCT excitation enhances the antibonding character between C and N atoms and the bonding character between two C atoms, which lengthens the C–N distance but shortens the C–C distance. (2) The Cu–N bond is shorter in the $^3A_2$ MLCT excited state than in the ground state. In the $^3A_2$ MLCT excited state, the diN ligand is negatively charged, as shown in Table I, because of one-electron excitation into its π^*_1 orbital. Thus, the donating ability of diN is enhanced in this excited state. Furthermore, the d_{xz} orbital is singly occupied in the $^3A_2$ excited state and, therefore, it can accept electrons, while in the ground state it is doubly occupied and, therefore, it cannot accept electrons. Consequently, electron donation from diN to Cu(I) is stronger in the MLCT excited state than in the ground state. Besides, exchange repulsion between d_{xz} and lone pairs of diN is smaller in this excited state than in the ground state because d_{xz} is singly occupied in this state but doubly occupied in the ground state. These factors lead to shortening of the Cu–N bond in the excited state. (3) The Cu–P bond is longer in this MLCT excited state than in the ground state. Electron donation from

---

(38) To compare various states correctly, optimization should be carried out for each electronic state. However, such a procedure is much time-comsuming. Thus, comparison was made on the geometry optimized at the $^1A_1$ ground state. Then, the geometry was optimized at the most stable $^3A_2$ state, and various states were compared on this optimized geometry. Furthermore, geometry optimization was also carried out at $^3A_1(d_{yz} \rightarrow \pi^*_1)$, which is expected to be the next stable state in pTd. However, this state is calculated to be less stable than $^2A_2$ at both the HF and MP2 levels (Table II). These calculations indicate that the $^3A_2$ state is the most stable MLCT excited state.

(39) (a) The Mulliken population of diN is 30.48 in the $^3A_2$ state and 30.52 in the $^3A_1$ state. Although the difference is small, this result supports that donation from diN to Cu(I) is stronger in the $^3A_2$ state than in the $^3A_1$ state. (b) Strictly speaking, the diN π orbital can donate electrons to the Cu d_{yz} orbital, even in the $^3A_1$ state. However, the diN π orbital lies slightly higher in energy than the diN lone pair orbital by only 0.16 eV. Thus, electron donation from diN lone pair to Cu d_{xz} in the $^3A_2$ state would be stronger than that from diN π to Cu d_{yz} in the $^3A_1$ state, owing to better overlap of the diN lone pair with Cu d_{xz}, and the main picture of electron distribution is determined by the donation from the diN lone pair to Cu d_{σ}. In fact, electron distribution described in ref 39a supports this consideration.

Chart III

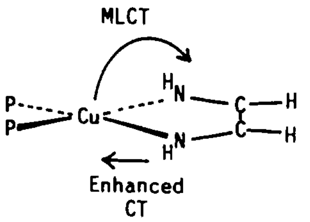

PH_3 to Cu(I) is enhanced in the $^3A_2$ MLCT excited state, which is consistent with the result that electron population of PH_3 is smaller in the excited state than in the ground state, as shown in Table I. In this excited state, however, electron donation from diN to Cu(I) is enhanced to a greater extent than that from PH_3 to Cu(I), as described above. Thus, the Cu–N bond becomes considerably strong, compared to the Cu–P bond, which lengthens the Cu–P distance due to the increased trans-influence effect of diN. (4) The PCuP angle in the Pl structure is also noted; this angle is 109° at the ground state but decreases to 91° upon MLCT excitation. The PCuP angle of 90° is favorable for electron donation from PH_3 to the d_{xz} orbital, which is singly occupied at this excited state. At the ground state, all d orbitals are doubly occupied, and therefore, no favorable situation appears even if the PCuP angle is 90° (vide supra).

Relative stabilities of the Pl and pTd structures are now interpreted in terms of electron occupation of the d orbitals in the $^3A_2$ excited state. In this state, the d_{xz} orbital is singly occupied but the d_{yz} orbital is doubly occupied. In the pTd structure, therefore, diN can donate electrons to the Cu d_{xz} orbital but PH_3 cannot. In the Pl structure, however, both diN and PH_3 can donate electrons to d_{xz}. This would be a main reason that Pl is more stable than pTd at the excited state.

Electron distribution and spin distribution of the $^3A_2$ MLCT excited state are important in understanding electronic structure of this excited state. In both the Pl and pTd structures, spin density on d_{xz} is calculated to be about 0.9e and spin densities on diN's p_y orbitals are summed up to about 0.9e, as shown in Table I. This result means that the excited electron is localized on the diN π^*_1 orbital and the electron configuration of the MLCT excited state can be represented as $(d_{xz})^1(\text{diN }\pi^*_1)^1$. Several experiments also indicate that the excited electron is localized on the dmp ligand in the lowest MLCT excited state of $[Cu(dmp)(PPh_3)_2]^+$.[40] It is mentioned here that although the $(d_{xz})^1(\text{diN }\pi^*_1)^1$ configuration corresponds to one-electron excitation from Cu d_{xz} to diN π^*_1, MLCT excitation decreases the atomic population of Cu to a lesser extent than 1.0e and increases the electron population of diN to a lesser extent than 1.0e. For instance, the Cu atomic population in the $^3A_2$ MLCT excited state is smaller by ca. 0.35e (Pl)–0.40e (pTd) than in the $^1A_1$ ground state, which mainly results from a significant decrease in the Cu d orbital population. On the other hand, electron populations of Cu s and p orbitals are larger in this state than in the ground state by ca. 0.35e and 0.60e, respectively. This electron distribution is easily understood as follows: one-electron excitation from Cu d_{xz} to diN π^*_1 yields one hole in the Cu d_{xz} orbital and adds one electron to the diN π^*_1 orbital, which lowers the Cu 4s and 4p orbitals in energy and raises diN's lone pair orbitals in energy. Thus, the MLCT excitation enhances electron donation from diN to the Cu 4s and 4p orbitals, as shown in Chart III. This would be a main reason for the electron distribution described above.

H_2O Coordination to Cu(I). H_2O coordination to Cu(I) is examined at both the $^1A_1$ ground state and $^3A_2$ MLCT excited one, where the geometry of $[Cu(diN)(PH_3)_2]^+$ is assumed not to change upon H_2O coordination.[41]

In the pTd structure at the ground state, O of H_2O does not approach Cu(I) but H of H_2O approaches N of diN, which corresponds to a hydrogen bond between solvent and diN. This interaction would be formed in any structure and any electronic state. In the pTd structure at the ground state, this interaction would be stronger than H_2O coordination to Cu(I). However, H_2O coordination to Cu(I) is investigated here. Thus, in the pTd structure at the ground state, only a Cu–O distance is optimized with the H_2O approaching angle fixed in order to prevent H_2O from approaching diN.[42] In the other cases, both the Cu–O distance and the approaching angle are optimized because H_2O can coordinate to Cu(I). The optimized structures of H_2O coordination are shown in Figure 3. The Cu–O distance is significantly long in the pTd structure at the ground state. Because this distance is too long compared to the usual coordinate bond, H_2O coordination is considered to be difficult in the pTd structure at the ground state. On the other hand, the Cu–O distance is calculated to be 2.379 Å in the Pl structure at the ground state, which is in the range of the usual coordinate bond. At the $^3A''$ MLCT excited state,[43] the Cu–O distance is 2.671 Å in the pTd structure and 2.299 Å in the Pl one. Again, the Cu–O distance of the Pl structure is in the range of the usual coordinate bond but that of the pTd one is longer than the usual coordinate bond.

The binding energy (BE) of H_2O coordination is given in Table III, together with changes in electron population caused by H_2O coordination. Apparently, BE is considerably small in the pTd structure at both the $^1A'$ ground state and $^3A''$ MLCT excited one, indicating weak coordination of H_2O to Cu(I) in this structure. At the ground state, BE in the Pl structure is larger than that in the pTd one, but it is still insufficient for the usual coordinate bond. At the $^3A''$ MLCT excited state, BE in the Pl structure is calculated to be 19.2 kcal/mol, which seems enough to form a coordinate bond. Thus, H_2O can coordinate to Cu(I) only in the Pl structure at the $^3A''$ MLCT excited state. The above results agree well with the quenching mechanism proposed by McMillin et al. (Scheme I);[3g,i] although solvent coordination to Cu(I) is difficult at the ground state, a solvent molecule can easily coordinate to Cu(I) in the Pl structure of $[Cu(diN)(PH_3)_2]^+$ at the $^3A_2$ MLCT excited state, yielding a five-coordinate complex.

Although BE and Cu–O distance have not been reported experimentally for H_2O coordination to $[Cu(NN)(PR_3)_2]^+$, H_2O coordination to $Cu^+(H_2O)_n$ (n = 0–3) has been investigated experimentally[44,45] and theoretically.[46] In H_2O coordination to $Cu^+(H_2O)_3$, the experimental value of BE is 15 ± 2[44] and 16.1 ± 0.2[45] kcal/mol and the theoretical one is 14.5 kcal/mol.[46] These values are larger than BE (12.9 kcal/mol) calculated for the Pl structure of $[Cu(diN)(PH_3)_2]^+$ at the ground state but smaller than BE (19.2 kcal/mol) calculated for the Pl structure of $[Cu(diN)(PH_3)_2]^+$ at the $^3A_2$ excited state. These results are easily explained as follows: BE at the ground state of the four-coordinate $[Cu(diN)(PH_3)_2]^+$ is smaller than in the three-coordinate Cu^+-

---

(40) (a) Smothers, W. K.; Wrighton, M. S. *J. Am. Chem. Soc.* **1983**, *105*, 1067. (b) Caspar, J. V.; Westmoreland, D.; Allen, G. H.; Bradley, P. G.; Meyer, T. J.; Woodruff, W. H. *J. Am. Chem. Soc.* **1984**, *106*, 3492. (c) McGarvey, J. J.; Bell, S. E.; Bechara, J. N. *Inorg. Chem.* **1986**, *25*, 4325. (d) Gordon, K. C.; McGarvey, J. J. *Chem. Phys. Lett.* **1989**, *162*, 117. (e) Gordon, K. C.; McGarvey, J. J. *Inorg. Chem.* **1991**, *30*, 2986.

(41) Full geometry optimization needs significantly long computational time. Because H_2O coordination to Cu(I) is not strong but rather weak, H_2O coordination is not considered to cause a significant geometry change in $[Cu(diN)(PH_3)_2]^+$. Thus, geometry optimization was carried out with the structure of $[Cu(diN)(PH_3)_2]^+$ fixed, to save computation time. This means that $[Cu(diN)(PH_3)_2]^+ \leftarrow OH_2$ is assumed to be square pyramidal in the $^3A_2$ MLCT excited state.

(42) The H_2O approaching angle was taken to be the same as that in the H_2O coordination to $[Cu(diN)(PH_3)_2]^+$, taking the pTd structure at the $^3A''$ MLCT excited state.

(43) The $^3A''$ state of $[Cu(diN)(PH_3)_2]^+ \leftarrow OH_2$ arises from the $^3A_2(d_{xz} \rightarrow \text{diN }\pi^*_1)$ MLCT excited state of $[Cu(diN)(PH_3)_2]^+$.

(44) Magnera, T. F.; David, D. E.; Stulik, D.; Orth, R. G.; Jonkman, H. T.; Michl, J. *J. Am. Chem. Soc.* **1989**, *111*, 5036.

(45) Holland, P. M.; Castleman, A. W. *J. Chem. Phys.* **1982**, *76*, 4195.

(46) Baushlicher, C. W.; Langhoff, S. R.; Partridge, H. *J. Chem. Phys.* **1991**, *94*, 2064. ab initio MO/MCPF calculations are carried out in this report.

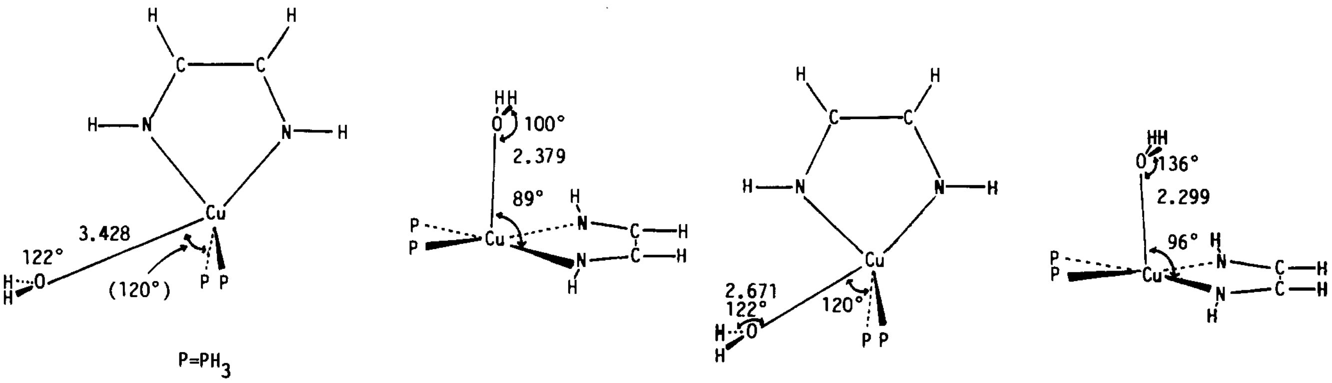

(A) $^1A_1$ Ground State

(B) $^3A_2$ MLCT Excited State

Figure 3. Optimized structures of H_2O coordination to Cu(I) (bond distances in Å and bond angles in deg). In parentheses is the assumed value, which is taken from the case where H_2O coordinates to the pTd structure of the $^3A_2$ MLCT excited state. See text for the reason.

Table III. Binding Energy (BE)[a] of H_2O Coordination to Cu(I) and Changes in Mulliken Populations[b] Caused by H_2O Coordination to Cu(II)

	$[Cu(diN)(PH_3)_2]^+ \leftarrow OH_2$				$[Cu(diN)(PH_3)_2]^{2+} \leftarrow OH_2$
	$^1A'$[c]		$^3A''$[d]		$^2A''$[e]
	pTd	Pl	pTd	Pl	Pl
			BE (kcal/mol)[a]		
MP2	(8.4)[f]	12.9[g]	6.1[h]	19.2[i]	31.4[j]
Cu	–0.014	–0.054	–0.057	–0.051	–0.070
PH_3	0.022	0.032	0.067	0.045	0.062
diN	0.013	0.032	0.013	0.060	0.053
H_2O	–0.043	–0.069	–0.091	–0.100	–0.107
			Spin Density		
d_{xz}			0.90	0.86	0.87
diN(π_y)			0.98	0.98	0

[a] $BE = E_t\{[Cu(diN)(PH_3)]^{+,2+}\} + E_t(H_2O) - E_t\{[Cu(diN)(PH_3)_2]^{+,2+} \leftarrow OH_2\}$. [b] Positive value means increase in Mulliken populations and vice versa. [c] $^1A'$ corresponds to $^1A_1$ of $[Cu(diN)(PH_3)_2]^+$. [d] $^3A''$ corresponds to $^3A_2$ of $[Cu(diN)(PH_3)_2]^+$. [e] $^2A''$ corresponds to $^2A_2$ of $[Cu(diN)(PH_3)_2]^{2+}$. [f] $E_t = -2584.7982$ hartrees. Parentheses mean that this value was obtained for a partially optimized structure. [g] $E_t = -2584.7791$ hartrees. [h] $E_t = -2584.6745$ hartrees. [i] $E_t = -2584.7049$ hartrees. [j] $E_t = -2584.3884$ hartrees.

$(H_2O)_3$ because BE decreases with increasing coordination numbers.[44–46] At the MLCT excited $[Cu(diN)(PH_3)_2]^+$, however, electron distribution of Cu is similar to that of Cu(II) (vide infra), which enlarges BE in the MLCT excited $[Cu(diN)(PH_3)_2]^+$, compared to BE of $Cu^+(H_2O)_3$.

Change in electron distribution caused by H_2O coordination is briefly discussed. Electron population of H_2O decreases upon its coordination to Cu(I), and its decrease is the greatest at the $^3A''$ state of the Pl structure. However, increasing order of BE does not coincide with decrease in electron population of H_2O. Furthermore, the atomic population of Cu slightly decreases upon H_2O coordination, while electron populations of PH_3 and diN slightly increase. This electron redistribution suggests that not only charge transfer from H_2O to Cu(I) but also polarization of $[Cu(diN)(PH_3)_2]^+$ occur upon H_2O coordination.

Comparison of the $^3A_2$ MLCT Excited $[Cu(diN)(PH_3)_2]^+$ with the Cu(II) Complex, $[Cu(diN)(PH_3)_2]^{2+}$. It is interesting to make a comparison between the MLCT excited $[Cu(diN)(PH_3)_2]^+$ and a similar Cu(II) complex, $[Cu(diN)(PH_3)_2]^{2+}$. The Pl structure of $[Cu(diN)(PH_3)_2]^{2+}$ is optimized at the $^2A_2$ state in which the d_{xz} orbital is singly occupied. This state is considered the ground state, because the Cu d_σ orbital is in general singly occupied in the Cu(II) complex. As shown in Figure 4, the Cu–N distance of $[Cu(diN)(PH_3)_2]^{2+}$ is longer than in the $^3A_2$ MLCT excited $[Cu(diN)(PH_3)_2]^+$ by ca. 0.1 Å, while the Cu–P distance of the former is slightly shorter than in the latter. In the $^3A_2$ MLCT excited $[Cu(diN)(PH_3)_2]^+$, the donating ability of diN is enhanced very much, as discussed above. As a result, electron donation from diN to Cu is greater in this MLCT excited $[Cu(diN)(PH_3)_2]^+$ than in $[Cu(diN)(PH_3)_2]^{2+}$, which leads to a stronger Cu–N bond in the former than in the latter. Because the strong coordinate bond of diN weakens the Cu–PH_3 bond in the $^3A_2$ MLCT excited $[Cu(diN)(PH_3)_2]^+$, $[Cu(diN)(PH_3)_2]^{2+}$ has a slightly shorter Cu–P bond but a slightly longer Cu–N bond than the $^3A_2$ MLCT excited $[Cu(diN)(PH_3)_2]^+$. The shorter Cu–P bond of $[Cu(diN)(PH_3)_2]^{2+}$ is consistent with the smaller electron population of PH_3 in this complex (Table I).

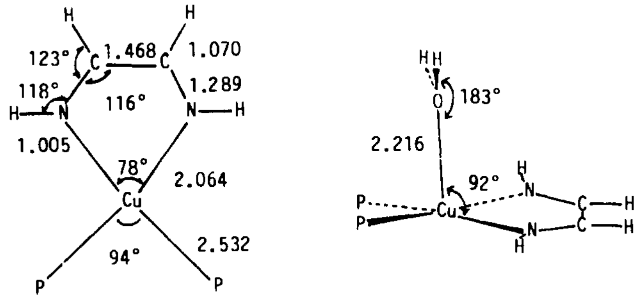

Figure 4. Optimized structures of $[Cu(diN)(PH_3)_2]^{2+}$ and H_2O coordination to it (bond distances in Å and bond angles in deg).

The geometry of the diN ligand is also different between these two complexes. The structure of diN in $[Cu(diN)(PH_3)_2]^{2+}$ differs little from the free diN molecule, while it considerably changes in the $^3A_2$ MLCT excited $[Cu(diN)(PH_3)_2]^+$ (vide supra). In the former, the diN π^*_1 orbital is unoccupied like in the free diN. Thus, large geometrical change does not take place. In the $^3A_2$ MLCT excited $[Cu(diN)(PH_3)_2]^+$, however, this orbital becomes singly occupied, which causes large geometrical change, as discussed above.

Although several differences are found between the $^2A_2$ state of $[Cu(diN)(PH_3)_2]^{2+}$ and the $^3A_2$ MLCT excited $[Cu(diN)(PH_3)_2]^+$, the Cu atomic population and the d_{xz} spin density are almost the same in these two complexes, as shown in Table I.

H_2O coordination to Cu(II) is investigated, then. Its BE is calculated to be 31.4 kcal/mol, which is much larger than in the $^3A_2$ MLCT excited $[Cu(diN)(PH_3)_2]^+$, and is enough to form a usual coordinate bond. Corresponding to this large BE value, the Cu–O distance (2.216 Å) is shorter than that in the $^3A_2$ MLCT excited $[Cu(diN)(PH_3)_2]^+$. It is worthy of note that although electron distribution around Cu is very similar in these two complexes, H_2O coordination to $[Cu(diN)(PH_3)_2]^{2+}$ is much stronger than in the MLCT excited $[Cu(diN)(PH_3)_2]^+$. This result is considered to arise from the difference in electron distribution of diN; in $[Cu(diN)(PH_3)_2]^{2+}$, diN is positively charged, but in the $^3A_2$ MLCT excited $[Cu(diN)(PH_3)_2]^+$, it is negatively charged. Such a negatively charged diN would disfavor H_2O coordination to Cu(I), compared to $[Cu(diN)(PH_3)_2]^{2+}$.

Concluding Remarks

$[Cu(diN)(PH_3)_2]^+$ takes the pTd structure at the $^1A_1$ ground state, which is more stable than the Pl one by ca. 16.5 kcal/mol. At the $^3A_2$ MLCT excited state, however, the Pl structure is more stable than the pTd one by only 4.1 kcal/mol. In the $^3A_2$ MLCT excited state, one α-spin electron is localized on the Cu d_{xz} orbital and the other α-spin electron is on the diN π^*_1 orbital. Thus, the electron configuration of the $^3A_2$ MLCT excited state can be described as $(d_{xz})^1(\text{diN } \pi^*_1)^1$.

H_2O coordination to Cu(I) is difficult at the $^1A_1$ ground state but easily occurs in the Pl structure of $[Cu(diN)(PH_3)_2]^+$ at the $^3A_2$ MLCT excited state. These results produce a theoretical support to the quenching mechanism of McMillin et al. proposed for the MLCT excited state of Cu(I) complexes.

The energy difference between pTd and Pl is only 4.1 kcal/mol at the $^3A_2$ MLCT excited state in the absence of the H_2O coordination. H_2O coordination enlarges this difference to 19.2 kcal/mol, which means that solvent coordination enhances the pTd → Pl geometry change in the MLCT excited state.

Finally, the $^3A_2$ MLCT excited state is compared with that for a similar Cu(II) complex, $[Cu(diN)(PH_3)_2]^{2+}$. Although H_2O coordination to Cu is stronger in $[Cu(diN)(PH_3)_2]^{2+}$ than in the MLCT excited $[Cu(diN)(PH_3)_2]^+$, electron and spin distributions around Cu are very similar in these two complexes.

Acknowledgment. MO calculations were carried out at the Computer Center of the Institute for Molecular Science (Okazaki, Japan) by using a Hitac S-820 computer. This work was supported by grant-in-aids from the Ministry of Education, Culture, and Science (No. 04243102).